IJCPE
Iraqi Journal of Chemical and Petroleum Engineering

Iraqi Journal of Chemical and Petroleum Engineering
Vol.17 No.3 (September 2016) 57- 73
ISSN: 1997-4884

University of Baghdad

Experimental Study and Mathematical Modelling of Zinc Removal by Reverse Osmosis Membranes

Ahmed Faiq Al-Alawy and Miqat Hasan Salih
Chemical Engineering Department, College of engineering, University of Baghdad

Abstract

In this study, aromatic polyamide reverse osmosis membranes were used to remove zinc ions from electroplating wastewater. Influence of different operating conditions such as time, zinc concentration and pressure on reverse osmosis process efficiency was studied. The experimental results showed, concentration of zinc in permeate increase with increases of time from 0 to 70 min, and flux of water through membrane decline with time. While, the concentrations of zinc in permeate increase with the increase in feed zinc concentration (10–300 mg/l), flux decrease with the increment of feed concentration. The raise of pressure from 1 to 4 bar, the zinc concentration decreases and the flux increase. The highest recovery percentage was found is 54.56% for reverse osmosis element, and the highest rejection of zinc was found is 99.49%. Experimental results showed that the concentrations of zinc ion in permeate was lower than the permissible limits (i.e. < 10 ppm). A mathematical model describing the process was investigated and solved by using MATLAB PROGRAM. Theoretical results were consistent with the experimental results approximately 90%.

Keywords: Heavy metals, Reverse osmosis, Zinc ions, Mathematical modelling.

Introduction

The world's population and the consequent desire for water supply increase, conservation of the invaluable and increasingly rare resource of water and sustainable development will require recycling and reuse. Then, water resource sustainability interests suggest exploring the possibility of reusing treated water as a promising source of water [1].

The development of industries such as tanneries, mining operations, paper industries, metal plating facilities, batteries, fertilizer industries, petroleum refining, photographic process industry, textile industry and pesticides etc., a considerable amount of wastewater containing heavy metals is discharged into the water, particularly in developing countries [2]. The high solubility in the aqueous environments, heavy metals can be absorbed by living organisms. They enter the food chain, high concentrations of heavy metals may accumulate in human body [3, 4]. Heavy metals are elements having atomic weights between 63.5 and 200.6, and a specific gravity greater than 5.0 [5]. Zinc organizes many

biochemical processes and is important for the physiological functions of living tissue. High concentrations of zinc cause prominent health problems, such as nausea, skin irritations, vomiting, anemia and stomach cramps. It is a trace element that is essential for human health [6]. The maximum contaminant level (standards) of zinc metal in water is 0.6-5 mg/l in Hong Kong SAR for Environmental Protection Department (EPD) [7], <10 mg/l for Egyptian Environmental Standards Law (93/62)/ and Decree (44/2000) [8] and 2 mg/l for the Iraq regulation limits [9]. Thus, heavy metals removal from discharge water becomes an increasingly important matter globally. Toxic heavy metals of particular interest in industrial wastewaters treatment involve zinc, chromium, mercury, copper, nickel, cadmium and lead [10, 11].

Different methods have been discussed for removing heavy metals from waters such as: coagulation, chemical precipitation, using ion exchange resins, flocculation, floatation, adsorption, electrochemical processes, and membrane methods [7, 12]. Membrane separation technologies have been specified to be a promising and feasible option for removal of heavy metal due to their ease of operation and high efficiency. Ultrafiltration (UF) and reverse osmosis (RO) are now being increasingly used for heavy metals removal from wastewater. Nanofiltration (NF) is less investigated intensively than RO for heavy metals removal because that RO is more effective to remove the divalent ions from wastewater than NF[13].

RO was the first membrane process to be widely commercialized. RO membranes are used to separate low molecular weight compounds and salts from water because they are highly permeable to water and highly impermeable to colloids, microorganisms, organic molecules and salts [14]. RO is one of the effective technologies to remove almost all pollutants, especially those with low concentrations. RO technology is also used today in large water treatment plants. It produces good quality of potable water from seawater and brackish water resources, reduce water salinity and improve polluted water sources for industrial applications. In addition, the application of series of RO membrane elements covers household units to produce higher quality of drinking water [15].

In this study, the effect of time, feed concentration and pressure on flux and permeate concentration, and comparison between experimental and theoretical results have been studied for reverse osmosis membranes to remove zinc ions from wastewater.

Mathematical Model

Spiral wound element is the most popular type of membrane element in use. Water passes through the element, some water passes into the permeate channel, resulting in continuously changing conditions over the length of the element [16].

1. Steady State Calculations

In the solution-diffusion model, the transport of solvent and solute are independent of each other. The flux of solvent through the membrane is linearly proportional to the pressure difference across the membrane [17]:

$$J_w = k_w\,(\Delta P - \Delta\pi) \qquad \ldots(1)$$

Where: J_w is the flux of water (l/m^2.h), k_w is the permeability coefficient of pure water (l/m^2.h.bar), ΔP is the applied pressure driving force (bar) and $\Delta\pi$ is the osmotic pressure of the solution (bar).

Solution osmotic pressure is related to its dissolved solute concentration and is predicted from Van't Hoff equation as:

$$\pi = \varphi\, i\, R_g\, T\, C \qquad \ldots(2)$$

Where: φ is the osmotic coefficient (dimensionless), i is the number of dissociated ions per molecule (Van't Hoff factor) (dimensionless), T is the temperature (K), R_g is the universal gas constant (l.bar/mole.K) and C is the concentration of solute (mg/l).

The Van't Hoff factor is inserted to more than deviations from ideal solution behavior that implicates finite volume occupied by molecules of solute and their mutual attraction as in Vander Waals attraction [18].
The solute flux through the membrane is proportional to the solute concentration difference across the membrane [17]:

$$J_s = k_s\, \Delta C \qquad \ldots(3)$$

Where: J_s is the solute mass flux (mg/m^2.h), k_s is the permeability coefficient of salt (m/h) and ΔC is the concentration gradient across membrane (mg/l).

And:

$$C_P = \frac{J_s}{J_w} \qquad \ldots(4)$$

Where: C_P is the concentration in permeate (mg/l).

By measuring the solute concentrations in feed solution (C_F) and also in permeate solution (C_P), the rejection is calculated from the rejection data as follows [11]:

$$R = \left(1 - \frac{C_P}{C_F}\right) \qquad \ldots(5)$$

Where: R is the solute rejection (dimensionless) and C_F is the concentration in feed solution.

At steady state, in the case with no accumulation of mass, the flux of solute to the membrane surface can be balanced by solute fluxes flowing away from the membrane and through the membrane as following[16]:

$$\frac{dM}{dt} = 0 = J_w C a - D_L \frac{dC}{dz} a - J_w C_P a \qquad \ldots(6)$$

Where: M is the solute mass (mg), t is the time (s), D_L is the solute diffusion coefficient in water (m^2/s), z is the distance perpendicular to the surface of membrane (m) and a is the surface area of membrane (m^2). Equation 6 can be not only applied at the surface of membrane but also at any plane in the boundary layer because the net flux of solute must be constant everywhere in the boundary layer to prevent the solute accumulation in that layer. Integrating Equation 6 across the thickness of the boundary layer with the boundary conditions: C(0) = C_M and $C(\delta_B) = C_{FC}$, where C_{FC} is the feed concentrate channel concentration and C_M is the membrane surface concentration.

$$D_L \int_{C_M}^{C_{FC}} \frac{dC}{C - C_P} = -J_w \int_0^{\delta_B} dz \qquad \ldots(7)$$

Integrate Equation 7 as:

$$\ln\left(\frac{C_M - C_P}{C_{FC} - C_P}\right) = \frac{J_w \delta_B}{D_L} \qquad \ldots(8)$$

$$\frac{C_M - C_P}{C_{FC} - C_P} = e^{\frac{J_w \delta_B}{D_L}} = e^{J_w / k_{Cp}} \qquad \ldots(9)$$

The concentration polarization is expression used to characterize the accumulation of rejected solute at the membrane surface so that the concentration of solute at the wall of membrane is greater than of the bulk

solution of feed. The convective flow of solute to the surface of membrane is greater than the diffusion back to the bulk feed solution; so that, the solute concentration at the wall of membrane increases [19]. Negative effects of concentration polarization involve [20]:

1- Changes in membrane separation properties.
2- Declines in the flux of water because of increased in osmotic pressure at the wall of membrane.
3- Enhanced fouling by colloidal or particulate materials in the feed which plug the surface of membrane and decrease the flux of water.
4- Increases in the flux of solute over the membrane due to increased concentration gradient across the membrane.
5- The solute precipitation if the concentration of surface exceeds its solubility limit, leading to particle fouling or scaling on membrane and reduced the flux of water.

Concentration polarization is defined as the ratio of the solute concentrations of membrane and feed concentrate channel as:

$$\beta = \frac{C_M}{C_{FC}} \qquad \ldots(10)$$

Where: β is the concentration polarization factor (dimensionless).

Combining Equation 10 with Equations 5 and 9 gives the following expression:

$$\beta = (1 - R) + R\ (e^{J_w/k_{Cp}}) \qquad \ldots(11)$$

Schock and Miquel [21] found that the mass transfer coefficient of concentration polarization could be calculated from equations below:

$$k_{Cp} = 0.023\ \frac{D_L}{d_H}\ (Re)^{0.875}\ (Sc)^{0.25} \qquad \ldots(12)$$

$$Re = \frac{\rho\ v\ d_H}{\mu} \qquad \ldots(13)$$

$$Sc = \frac{\mu}{\rho\ D_L} \qquad \ldots(14)$$

Where: $k_{Cp} = D_L/\delta_B$ is the mass transfer coefficient of concentration polarization (m/h), d_H is the hydraulic diameter (m), Re is the Reynold number (dimensionless), Sc is the Schmidt number (dimensionless), v is the velocity in the feed channel (m/h), ρ is the density of feed water (kg/m^3) and μ is the dynamic viscosity of feed water (kg/m.s).

As shown in Figure 1 the center plane of a differential slice of membrane performs the surface of membrane. The feed concentrate channel overhead the membrane, the permeate channel below the membrane.

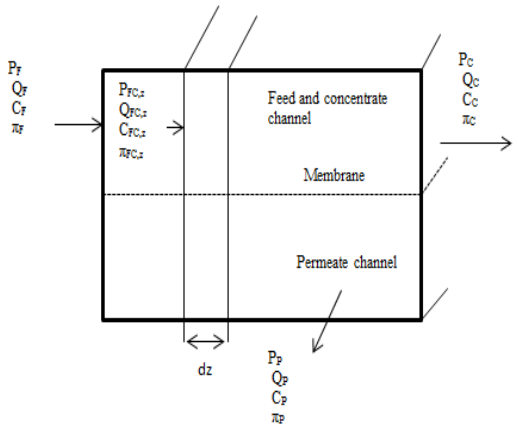

Fig. 1: Differential slice of membrane element

The water and solute fluxes are expressed by Equations 1 and 3, but the concentration differential, osmotic pressure differential and applied pressure differential rely on the position in the pressure vessel [16]:

$$J_{w,z} = k_w\ (\Delta P_z - \Delta\pi_z) = k_w\ \left[\left(P_{FC,z} - P_{P,z}\right) - \left(\pi_{M,z} - \pi_{P,z}\right)\right] \qquad \ldots(15)$$

$$J_{S,z} = k_S\ (\Delta C_z) = k_S\ \left(C_{M,z} - C_{P,z}\right) \qquad \ldots(16)$$

Where: $C_{M,z}$ is the concentration at the surface of membrane, $C_{M,z} = \beta_z\, C_{FC,z}$ and $\pi_{M,z}$ is the osmotic pressure at the surface of membrane.

The flow of permeate and flow of mass of solute through the membrane are equal to the flux multiply by the area of membrane for the differential element. The accumulative water and solute transfer across the membrane is predicted by integrating the flow between the feed end and the position *z* in the pressure vessel, as:

$$Q_{P,z} = \int_0^z J_{w,z}\, w\, dz \qquad \ldots(17)$$

$$M_{s,z} = \int_0^z J_{s,z}\, w\, dz \qquad \ldots(18)$$

Where: w is the width of feed concentrate channel (m) and $M_{s,z}$ is the solute mass transferred (mg/s).

Flow rate of water in the feed concentrate channel decreases as the permeate is produced. At any point in the channel the flow rate can be predicted by [16]:

$$Q_{FC,z} = Q_F - Q_{P,z} \qquad \ldots(19)$$

The concentration of solute in the feed concentrate channel can be calculated by doing a mass balance on solute as:

$$C_{FC,z} = \frac{Q_F C_F - M_{s,z}}{Q_{FC,z}} \qquad \ldots(20)$$

The flux of water and solute are influenced by solute concentration at the membrane surface and concentration polarization. Both velocity and flux are changing, β must be determined by Equation 11 as a function of position, as the following equation:

$$\beta_z = R\left(e^{\frac{J_{w,z}}{k_{CP,z}}}\right) + (1 - \mathrm{R}) \qquad \ldots(21)$$

The velocity in the feed concentrate channel which mass transfer coefficient k_{Cp} depends on it can be calculated from the following equation:

$$\upsilon_z = \frac{Q_{FC,z}}{hw} \qquad \ldots(22)$$

Where h is the height of feed concentrate channel (m).

The concentration of solute at the surface of membrane as a function of position expressed as:

$$C_{M,z} = \beta_z\, C_{FC,z} \qquad \ldots(23)$$

The feed channel pressure drops because of the head loss, head loss changes across the length of the membrane. Turbulent conditions are maintained, so head loss in the channel is given by the expression:

$$h_L = \delta_{HL}\, \upsilon^2 L \qquad \ldots(24)$$

Where: h_L is the feed concentrate channel head loss (bar), δ_{HL} is the head loss coefficient (bar.s^2/m^3), υ is the velocity of water in feed concentrate channel (m/s) and L is the length of the channel (m).

The concentration of permeate can be determined from the ratio of the fluxes of solute and water per Equation 4 as:

$$C_{P,z} = \frac{J_{s,z}}{J_{w,z}} \qquad \ldots(25)$$

2. Unsteady Steady State Calculations

Recovery can be expressed as the volume of permeate divided by the initial volume of feed. This expression applied in batch concentrating mode. For the overall system, the expression is [22]:

$$Y\% = \frac{V_P}{V_F^o} * 100\% \qquad \ldots(26)$$

Where: $Y\%$ is the recovery (percentage), V_P is the volume of permeate (l) and V_F^o is the initial feed volume (l).

Reverse osmosis unit in continuous operation consists of a tank for feed, a tank for product and the membrane element. The concentrate is recycled back to the tank of feed and the permeate is separately collected in the product tank as shown in Figure 2 [23].

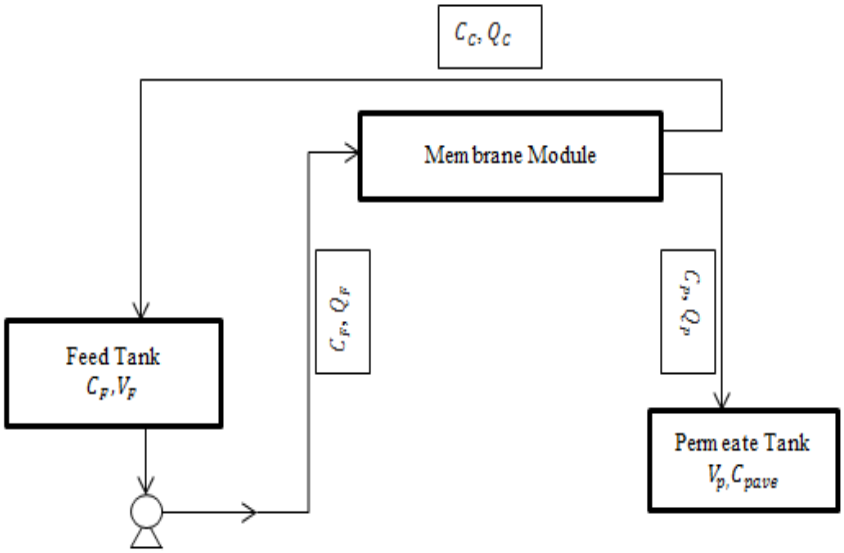

Fig. 2: Reverse osmosis system

Material balance equation applied for the product tank as**:**

$$Q_P C_P = \frac{d(V_P C_{Pave})}{dt} \quad \ldots(27)$$

C_{Pave} is the product average concentration (mg/l).

Expansion of equation 27 yields:

$$Q_P C_P = V_P \frac{dC_{Pave}}{dt} + C_{Pave} \frac{dV_P}{dt} \quad \ldots(28)$$

Initial conditions, at t=0, V_P=0, C_{Pave}=C_P=0. The variation in the product volume corresponds to the production rate of membrane as:

$$\frac{dV_P}{dt} = Q_P \quad \ldots(29)$$

Substitution to Equation 28:

$$\frac{dC_{Pave}}{dt} = \frac{Q_P(C_P - C_{Pave})}{V_P} \quad \ldots(30)$$

Material balance on the membrane element gives:

$$Q_F C_F = Q_P C_P + Q_C C_C \quad \ldots(31)$$

Analogous material balance equation can be obtained around the feed tank:

$$Q_C C_C - Q_F C_F = \frac{d(V_{Ft}\, C_{Ft})}{dt} \quad \ldots(32)$$

Developing this equation gives:

$$-Q_P C_P = V_{Ft} \frac{dC_{Ft}}{dt} + C_{Ft} \frac{dV_{Ft}}{dt} \quad \ldots(33)$$

Where, V_{Ft} is the volume in the tank of feed at a time t, with a concentration in the tank C_{Ft}. The tank of feed is assumed well mixed [22] so:

$$V_{Ft} = V_F \quad \ldots(34)$$

And:

$$C_{Ft} = C_F \quad \ldots(35)$$

The variation in the feed tank volume with time corresponds to the production rate as:

$$-\frac{dV_F}{dt} = Q_P \quad \ldots(36)$$

Integrating equation 36 with the initial condition: t=0, $V_F = V_F^o$

$$V_F = V_F^o - Q_P\, t \quad \ldots(37)$$

Substituting these expressions in Equation 33:

$$\frac{dC_F}{dt} = \frac{Q_P(C_F - C_P)}{(V_F^o - Q_P\, t)} \quad \ldots(38)$$

Knowing that the system of interest is closed, the conservation of mass reveals that the solute mass in feed tank at initial time is equal to the sum of various streams and tank:

$$V_P = \frac{V_F^o(C_F - C_F^o)}{(C_F - C_{Pave})} \quad \ldots(39)$$

Substituting V_P by its expresssion in Equation 30:

$$\frac{dC_{Pave}}{dt} = \frac{Q_P(C_P - C_{Pave})}{V_F^o(C_F - C_F^o)}(C_F - C_{Pave}) \quad \ldots(40)$$

Equation 38 and 40 are the outcome of material balances on the product tank, feed tank, and membrane element. The solution of this set of ordinary differential equations requires the values of C_P and Q_P. C_P and Q_P are obtained from the steady state equations 4 and 17 as initial values for the ordinary differential equations when the concentration and product rate of permeate change with position of module. The solution of Equation 38 gives the concentration of feed as function of time. The solution of Equation 40 gives the solute average concentration in product tank and the volume of water by Equation 39. The equations of the mathematical model can be solved by using MATLAB PROGRAM.

Experimental Work

Synthetic wastewater containing the desired concentrations of Zn^{+2} were prepared by dissolving the desired amount of zinc chloride ($ZnCl_2$, Minimum assay 97%, M.W. 136.28, CAS-NO. 7646-85-7 UN 2331, INDIA) in deionized water of conductivity 1-2 µs/cm.

Commercially spiral-wound ultra low pressure aromatic polyamide reverse osmosis membrane element is used in this work, can work under ultra low pressure to attain as high permeate flow rate and salt rejection as low pressure membrane element can, the specifications of this module are given in Table 1.

Schematic diagrams of lab-scale RO system used in these experiments are shown in Figure 3. Feed solution was prepared in feed vessel by dissolving the $ZnCl_2$ in 8 liter of deionized water. Pressure gauge (Range: 0-10 bar) is used in the feed line to indicate the operating pressure, the feed solution drawn from the feed vessel by centrifugal pump (Model: 15 GR-18, Rated power: 150 W, Rated voltage: 220-240 V, Rated current: 0.58 A, Rated speed: 2860 r/min, Frequency: 50/60 Hz, Highest head: 15 m, Rated head: 10 m, Max. capacity: 25 l/min, Rated capacity: 10 l/min, Insulation class: B) then the solution is introduced into the spiral-wound reverse osmosis element by means of a high pressure pump (Model: HF-6050, Max. outlet pressure: 125 psi, Open flow: 1.2 l/min, VOLTS: 24 VDC, AMPS: 0.26 A). The feed temperature was varied by submersible electrical coil (Rated power: 1000 W, Rated voltage: 220V). The feed flow rate was controlled by rotameter (Range: 10-100 l/h) and keeping constant at 40 l/h. The concentrate stream is recycled to

the feed vessel and mixed with the feed stream. The water flux was obtained by dividing the permeate volume by the product of effective area of membrane and time. The concentration of heavy metal ion (Zn^{+2}) was measured by an atomic absorption spectrometry (Buck 210/211, U.S.A., Perkin Elmer, Sr.Nr:1159 A). After recording the results, the solution was drained by a drain valve and the system was washed by deionized water.

Table 1: Specification of reverse osmosis element

Model	VONTRON-ULP 1812-50
Type of membrane	Ultra low pressure aromatic polyamide reverse osmosis membrane element
Active membrane area, m^2	0.36
Average permeated flow, m^3/d	0.19
Stable rejection rate, %	97.5
Minimum rejection rate, %	96
Testing pressure, Mpa	0.41
Concentration of testing solution (NaCl), ppm	250
pH of testing solution	7.5
Recovery of single membrane element, %	15
Maximum working pressure, Mpa	2.07
Maximum feed water temperature, °C	45
Maximum feed water SDI	5
Free chlorine concentration of feed water, ppm	<0.1
pH range of feed water during continuous operation	3-10
pH range of feed water during chemical cleaning	2-12

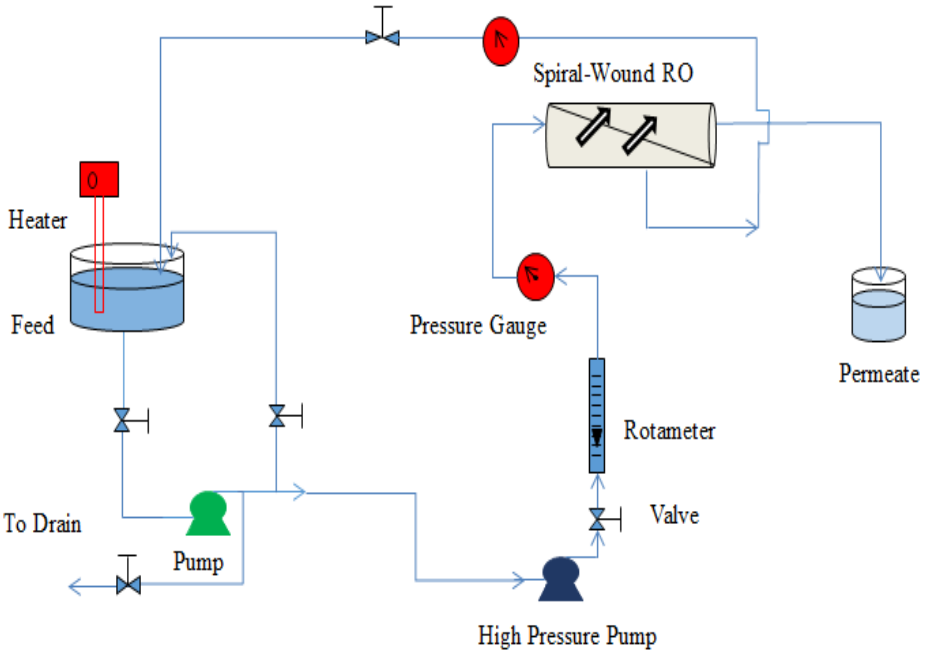

Fig. 3: Schematic diagram of lab-scale RO system

Results and Discussion

The aromatic polyamide membrane permeability (k_w) for pure water was experimentally determined by a hydraulically low pressure RO process. The pure water flux through the

membrane was determined with range of pressures according to Equation 1 when $\Delta\pi = 0$.
As shown in Figure 4, the data shows a linear relationship between water flux and driving force. Aromatic polyamide compound membrane permeability for pure water is determined from the slope of this curve, the value of k_w was obtained 6.736 l/m^2.bar.h.

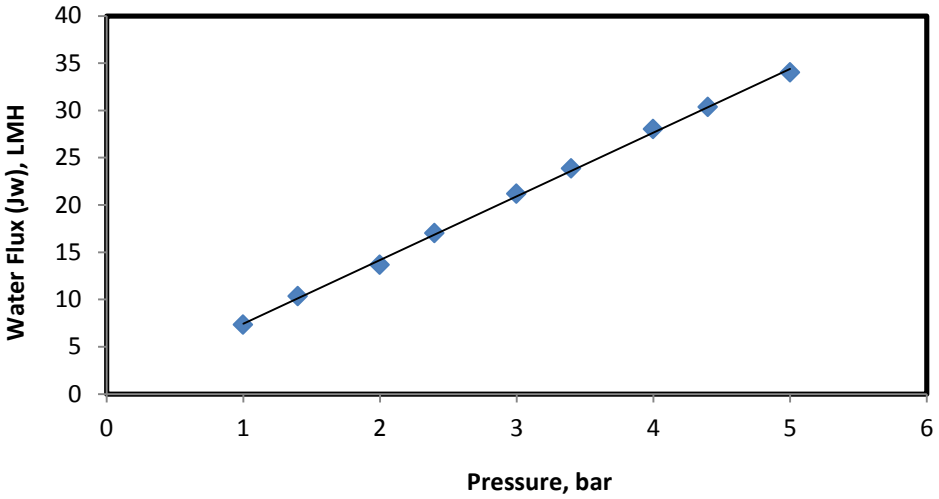

Fig. 4: Operating pressure vs. water flux (Q_F = 30 l/h, T = 26 ^oC and t=10 min)

The membrane permeability (k_s) for salt ($ZnCl_2$) was experimentally determined under a range of feed concentrations according to Equation 3.

As shown in Figure 5, the data show a linear relationship between mass flux of solute and driving force. Membrane permeability for salt is determined from the slope of this curve, the value of k_s was obtained 2.498*10^{-4} m/h.

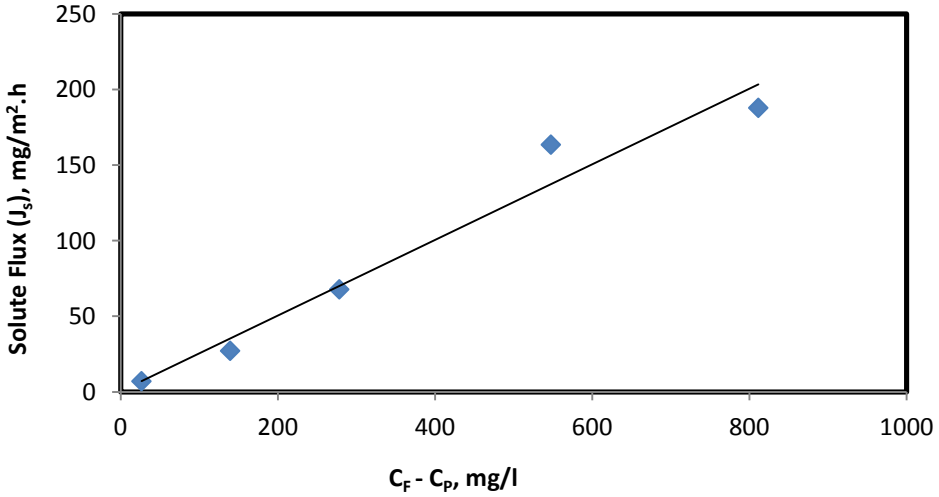

Fig. 5: Concentration difference vs. solute flux (QF=40 l/h, T=26 ^oC , t=30 min and P=2 bar)

Figure 6 show the effect of time on the concentration of zinc ion in permeate. The heavy metal ions concentration in the product gradually increased with the increase in operating time. This behavior can be explained by the increase of the feed concentration with time in the recirculation mode led to increase in concentration polarization and this cause an increase in the zinc

passage, this behavior is agreement with Xiuzhen [13]. The first 30 minutes resulted in the increase in permeate concentration of 17.72% and the final 40 minutes resulted in the increase in permeate concentration of 52.58%.

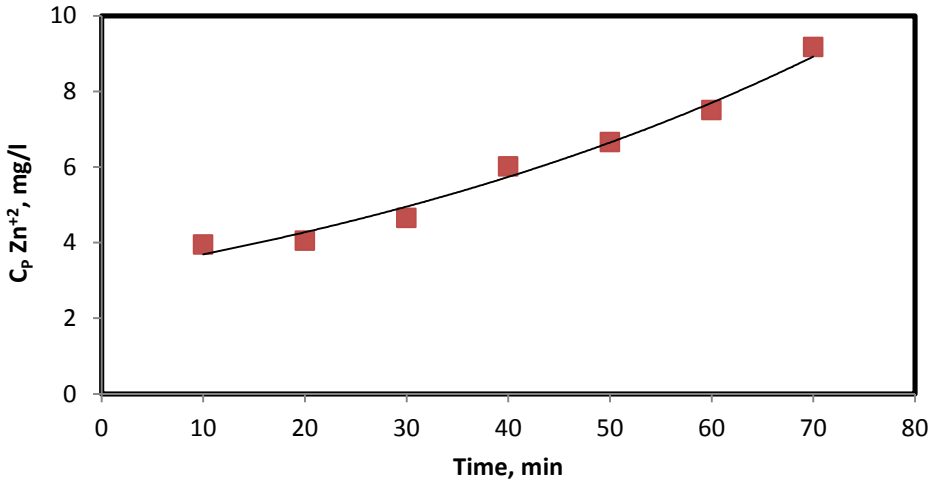

Fig. 6: Effect of operating time on permeate concentration of zinc ions (Q_F = 40 l/h, T = 26 ^oC, pH = 6, P = 2 bar, C_{Zn+2}=300 mg/l)

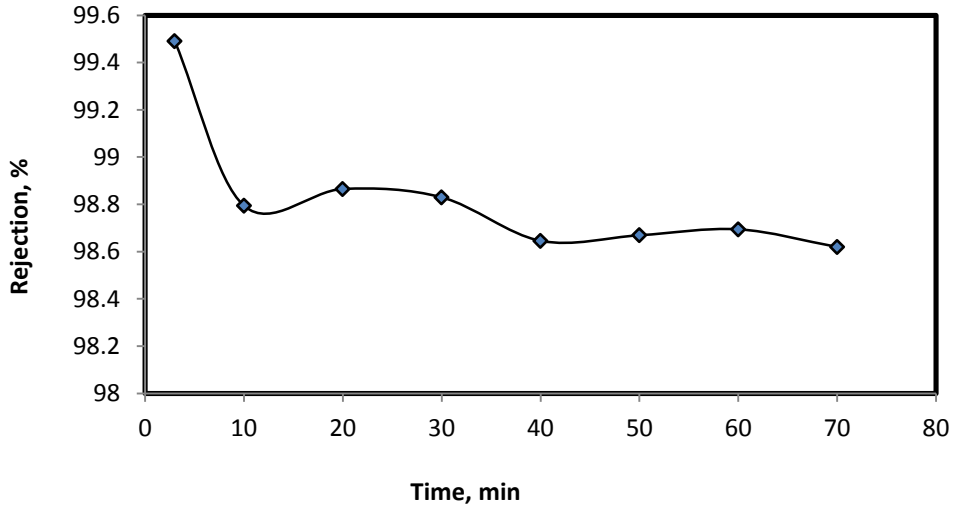

Fig. 7: Effect of operating time on rejection of zinc ions (Q_F = 40 l/h, T = 26 ^oC, pH = 6, P = 2 bar, C_{Zn+2}=300 mg/l)

As shown in Figure 7 the rejection rates of zinc ions have been randomly decreased and increased in spite of that the concentration of zinc ions in permeate has been increased with time, this behavior due to the increase in feed concentration (feed concentration has been changed with time) because of the recirculation mode. The rejection for zinc ion at first three minutes when the feed concentration approximately constant (300 mg/l) is 99.49%.

Figure 8 shows the effect of time on flux. It can be easily observed that the flux from reverse osmosis unit decrease with increase in operating time. The continuous decrease of the flux was mainly due to the gradual increase in the viscosity of solution

and to heavy metal deposition onto the membrane surface with increasing feed concentration and osmotic pressure gradually, which led to further membrane fouling and severe concentration polarization. Resistance against water flux through the membrane increased due to the boundary layer on the membrane surface formed by heavy metals. Furthermore, increasing osmotic pressure because of concentration polarization led to a decrease in the driving force through the membrane. This behavior is agreement with Xiuzhen and Zhi [13, 24]. The increase in time to 70 min resulted in the flux decline of 6.226%.

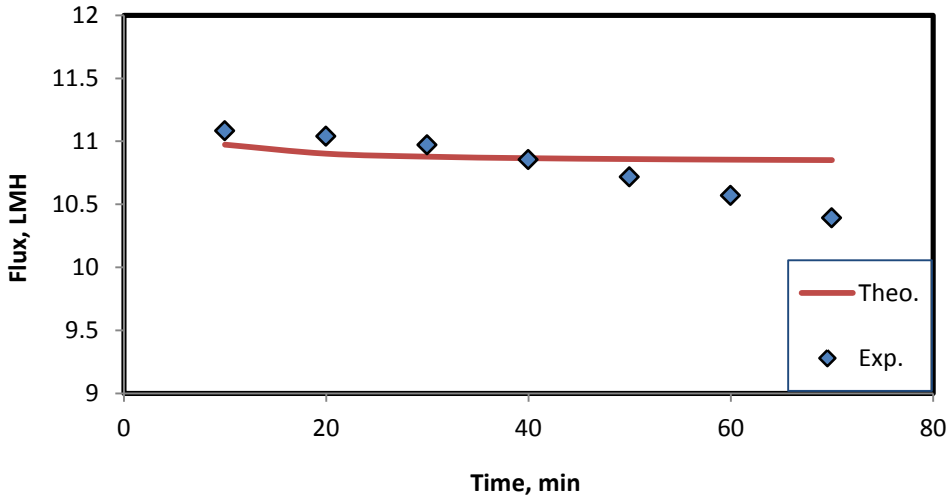

Fig. 8: Effect of operating time on flux (Q_F = 40 l/h, T = 26 ^oC, pH = 6, P = 2 bar, C_{Zn+2}=300 mg/l)

Figure 9 shows the effect of time recovery percentage of permeate. The recovery percentage increase according to equation 26 because the accumulation volume of permeate has been increased as time increased. The increase in time to 70 min resulted in the increase of water recovery from 8.3125 to 54.5625%.

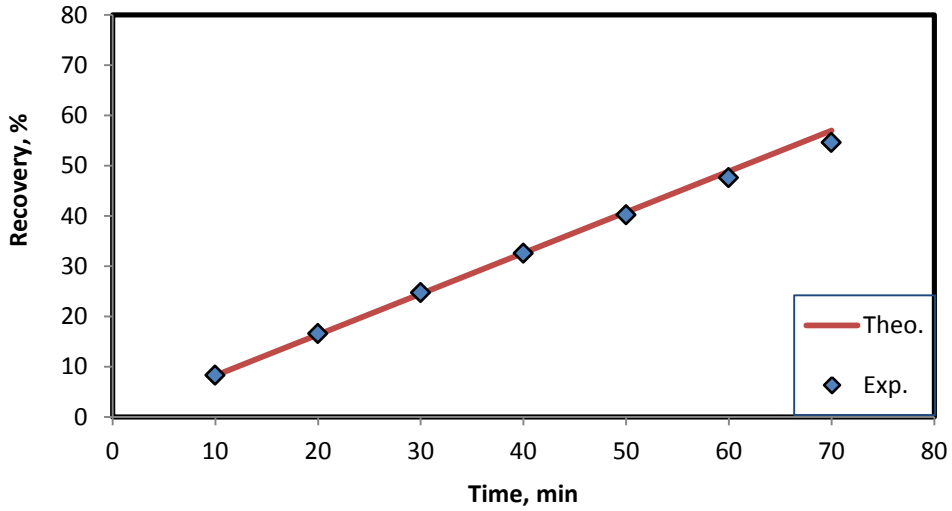

Fig. 9: Effect of operating time on recovery percentage (Q_F = 40 l/h, T = 26 ^oC, pH = 6, P = 2 bar, C_{Zn+2}=300 mg/l)

Figure 10 shows the values of final feed vessel concentration change with time. It can be observed that the feed concentration increase with increase in operating time. This behavior was due to the recirculation mode (concentrate stream recycled to the feed stream).

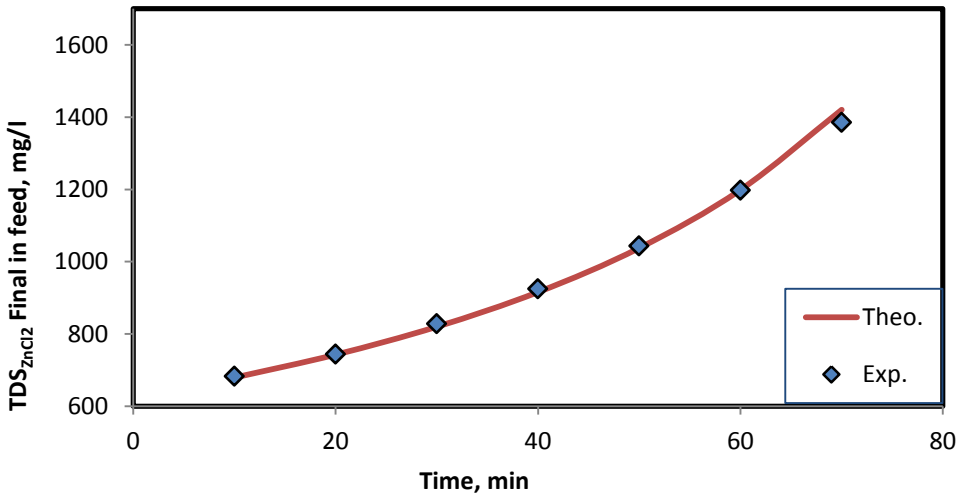

Fig. 10: Effect of operating time on final feed concentration (Q_F = 40 l/h, T = 26 ^oC, pH = 6, P = 2 bar, $C_{Zn^{+2}}$=300 mg/l

As shown in Figure 11 zinc concentration in permeate has been increased as the feed concentration increased, this behavior is agreement with Kyu [25]. The increase in feed concentration ion from 10 to 300 mg/l resulted in the increase of permeate concentration from 0.19 to 4.63 mg/l.

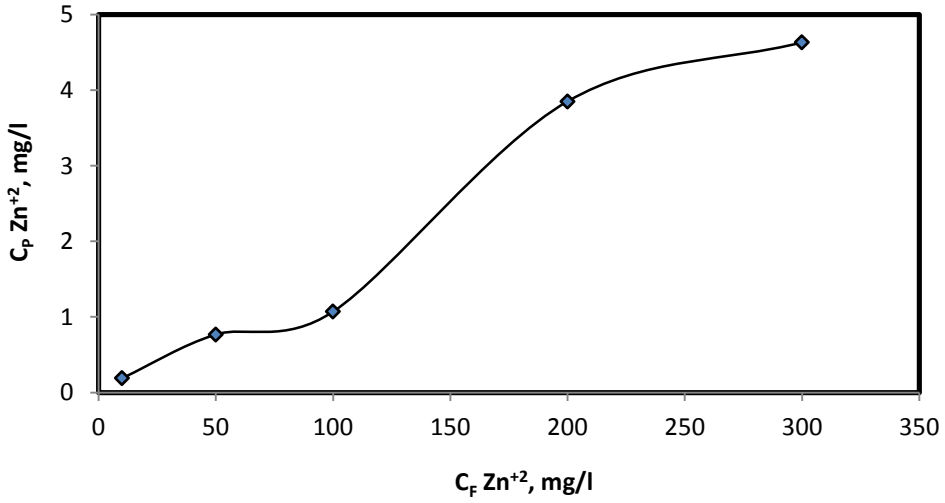

Fig. 11: Effect of feed concentration on permeate concentration of zinc ions (Q_F = 40 l/h, T = 26 ^oC, pH = 6, P = 2 bar, t=30 min)

It is clear from Figures 12 and 13 that the permeate flux and recovery have been decreased with increasing feed concentration. This behavior due to increase in osmotic pressure, decrease of the effective membrane pore size due to adsorption of solute on the membrane surface and the effect of concentration polarization, this behavior is agreement with Kyu [25]. The decrease in recovery according to decrease in flux. The increase in feed

concentration ion from 10 to 300 mg/l resulted in the decrease of recovery from 30.81% to 24.5% and flux from 13.694 to 10.889 LMH.

Figure 14 show the values of final feed vessel concentration. It can be observed that the feed concentration increase with increase in ion feed concentration. This behavior due to the recirculation mode (concentrate stream recycled to the feed stream).

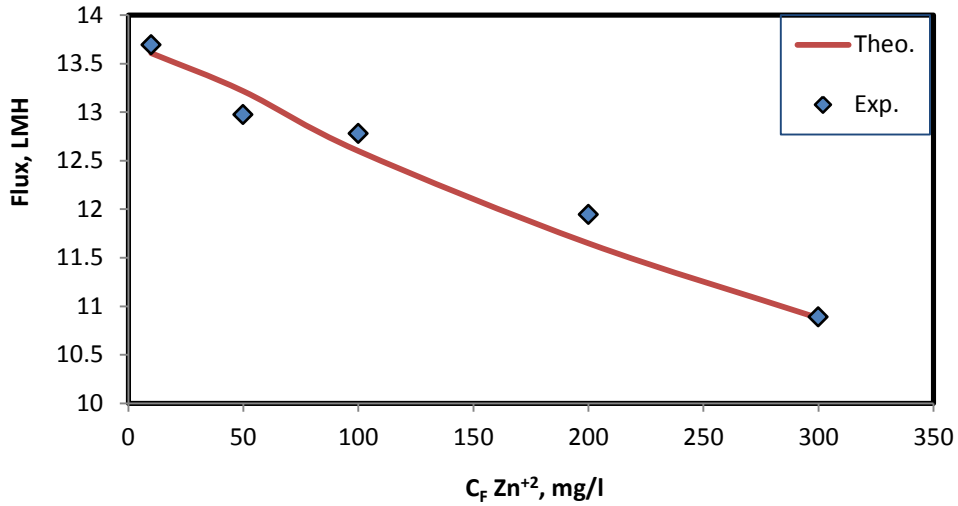

Fig. 12: Effect of feed concentration on flux (Q_F = 40 l/h, T = 26 ^oC, pH = 6, P = 2 bar, t=30 min)

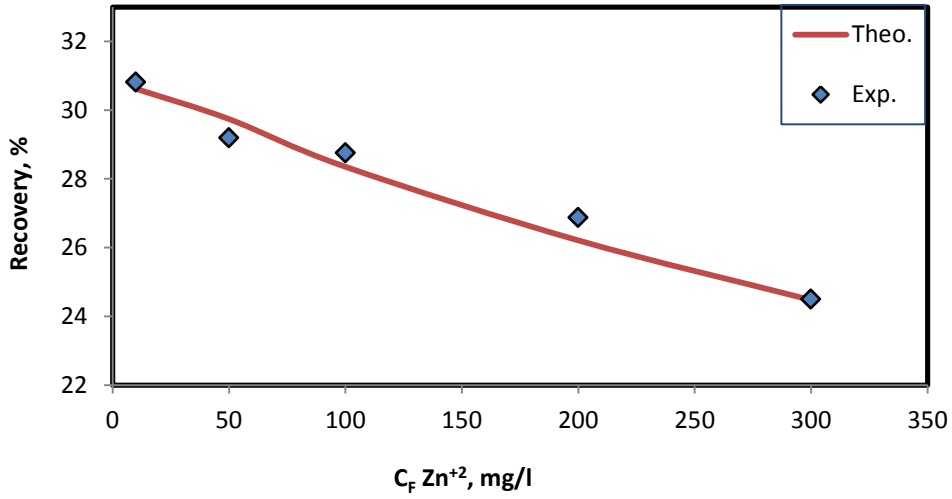

Fig. 13: Effect of feed concentration on recovery percentage (Q_F = 40 l/h, T = 26 ^oC, pH = 6, P = 2 bar, t=30 min)

Figure 15 shows that the zinc concentration in permeate has been decreased with increasing applied pressure which can be explained by the following: The decrease in concentration of ion in permeate with raise in pressure could be because of at higher pressure the preferential sorption of the membrane element for pure water has been increased and the average pore size on the membrane surface has been decreased, also due to increase in flux with increasing applied pressure. In other words, at low pressure the solute diffusive transport through membrane is higher than that of convective transport. As the applied pressure increases, convective

transport becomes more important which make it possible to decrease the concentration of ion in permeate, this behavior is agreement with Xijun [26].

The increase in pressure from 1 to 4 bar resulted in the decrease of permeate concentration of zinc ion of 49.927%.

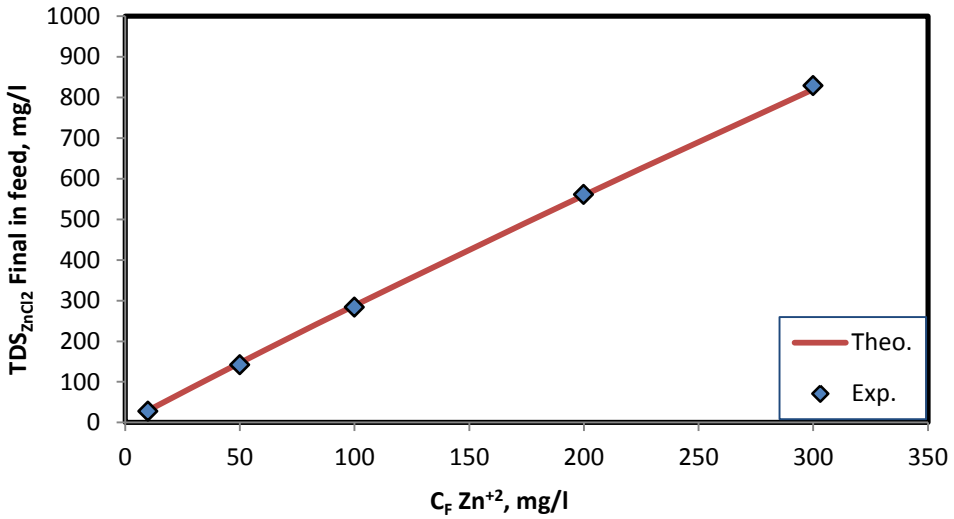

Fig. 14: Effect of feed concentration on final feed concentration (Q_F = 40 l/h, T = 26 ^oC, pH = 6, P = 2 bar, t=30 min)

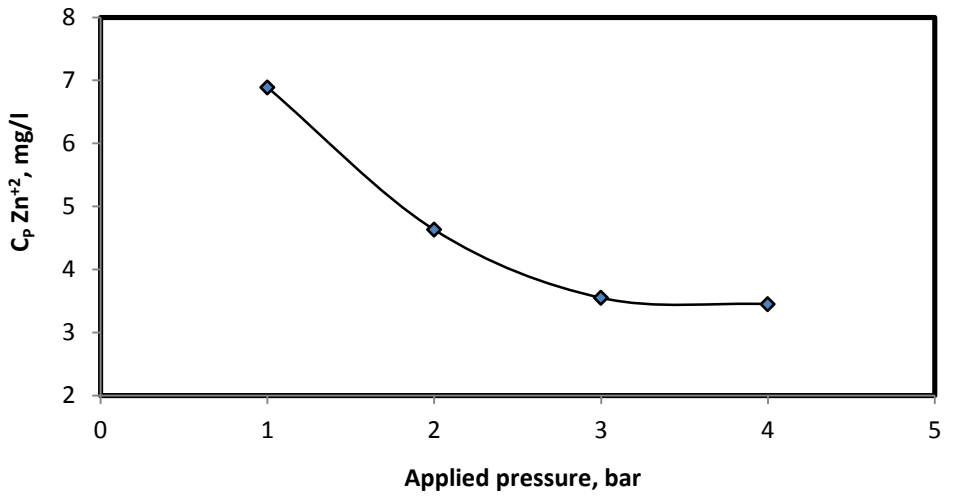

Fig. 15: Effect of applied pressure on permeate concentration of zinc ions (Q_F = 40 l/h, T = 26 ^oC, pH = 6, C_{Zn+2}=300 mg/l, t=30 min)

As shown in Figures 16 and 17 the permeate flux and recovery has been increased linearly with increasing applied pressure, this means that there is a little effect of concentration polarization in the membrane module. This behavior can be explained by the permeability equation of solution diffusion model (Equation 1), this behavior is agreement with Jae [27].

The increase in applied pressure from 1 to 4 bar resulted in the increase of flux of 311.979%.

Figure 18 shows the values of final feed vessel concentration. It can be observed that the feed concentration increase with increase in applied pressure. This behavior due to the recirculation mode (concentrate stream recycled to the feed stream).

It can be seen from Figures 8, 9, 10, 12, 13, 14, 16, 17 and 18 that the model prediction values are in good agreement with the experimental results.

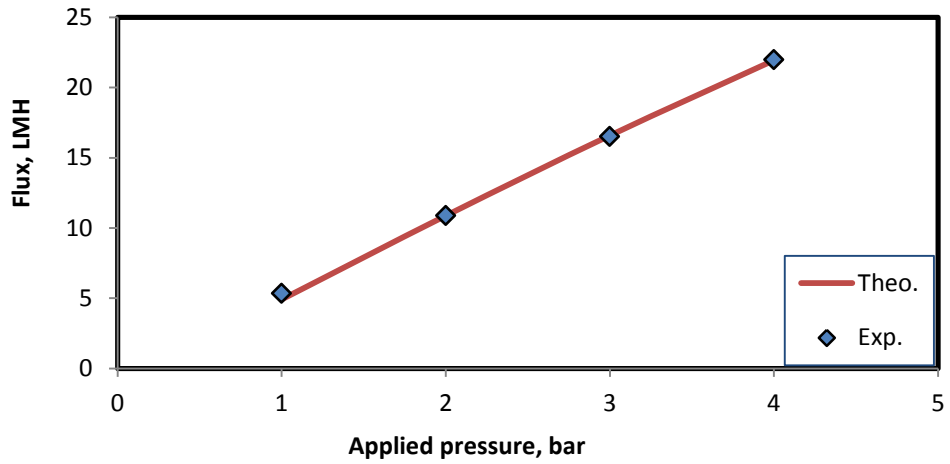

Fig. 16: Effect of applied pressure on flux (Q_F = 40 l/h, T = 26 ^oC, pH = 6, C_{Zn+2}=300 mg/l, t=30 min)

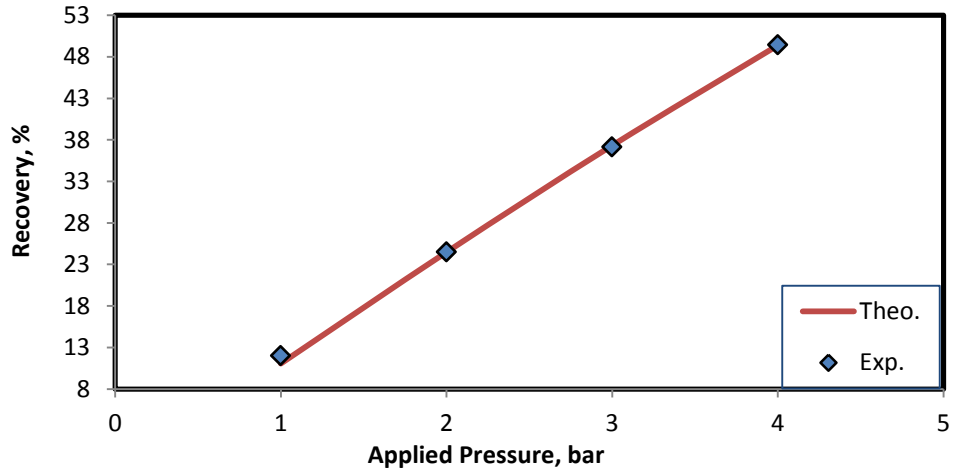

Fig. 17: Effect of applied pressure on recovery percentage (Q_F = 40 l/h, T = 26 ^oC, pH = 6, C_{Zn+2}=300 mg/l, t=30 min)

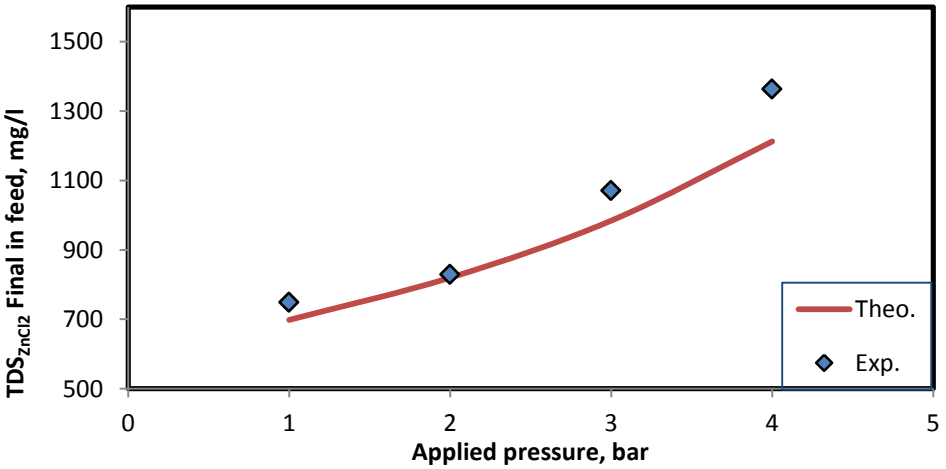

Fig. 18: Effect of applied pressure on final feed concentration (Q_F = 40 l/h, T = 26 ^oC, pH = 6, C_{Zn+2}=300 mg/l, t=30 min)

Conclusion

The aromatic polyamide reverse osmosis membrane gives a high efficiency for removal of zinc ions and it has allowed permeation of zinc ion to the lower than permissible limits. The rejection percentage for zinc ion was high (i.e. > 98%) for most experiments in this research. The recovery percentage for reverse osmosis element was 54.56% during the time of 70 minutes. The polyamide membrane permeability for zinc chloride is $2.498*10^{-4}$ m/h. The theoretical flux values calculated from mathematical model are in a good agreement with the experimental results.

References

1. Salem Alzahrani, A.W. Mohammad, N. Hilal, Pauzi Abdullah, Othman Jaafar, "*Comparative study of NF and RO membranes in the treatment of produced water—Part I: Assessing water quality*", Desalination, **Vol.315**, p.p.18-26, (2013).
2. Fenglian Fu, Qi Wang, "*Removal of heavy metal ions from wastewaters: A review*", Journal of Environmental Management, **Vol.92**, p.p.407-418, (2011).
3. M.A. Barakat, "*New trends in removing heavy metals from industrial wastewater*", Arabian Journal of Chemistry, **Vol.4**, p.p.361–377, (2011).
4. Tonni Agustiono Kurniawan, Gilbert Y.S. Chana, Wai-Hung Loa, Sandhya Babel, "*Physico–chemical treatment techniques for wastewater laden with heavy metals*", Chemical Engineering Journal, **Vol.118**, p.p. 83–98, (2006)
5. N.K. Srivastava, C.B. Majumder, "*Novel biofiltration methods for the treatment of heavy metals from industrial wastewater*", Journal of Hazardous Materials, **Vol.151**, p.p.1-8, (2008).
6. M. Ahmaruzzaman, " *Industrial wastes as low-cost potential adsorbents for the treatment of wastewater laden with heavy metals*", Advances in Colloid and Interface Science, **Vol.166**, p.p. 36–59, (2011).
7. R. M. Abhanga, K.S. Wani, V.S. Patil, B.L. Pangarkar, S.B. Parjane, "*Nanofiltration for Recovery of Heavy Metal Ions from Waste Water - A Review*", International Journal of Research in Environmental Science and Technology, **Vol.3(1)**, p.p.29-34, (2013).
8. R. Abdel Wahaab, A.K. Moawad, Enas Abou Taleb,Hanan S. Ibrahim and H.A.H. El-Nazer, "C*ombined Photocatalytic Oxidation and Chemical Coagulation for Cyanide and Heavy Metals Removal from Electroplating Wastewater*", World Applied Sciences Journal, **Vol.8 (4)**, p.p.462-469, (2010).
9. Ministry of Iraqi Environment.
10. Wen-Ping Zhu, Jie Gao, Shi-Peng Sun, Sui Zhang, Tai-Shung Chung, "*Poly(amidoamine) dendrimer (PAMAM) grafted on thin film composite (TFC) nanofiltration (NF) hollow fiber membranes for heavy metal removal*", Journal of Membrane Science, **Vol.487**, p.p. 117–126, (2015).
11. Cristina-Veronica Gherasim, PetrMikulášek, "*Influence of operating variables on the removal of heavy metal ions from aqueous solutions by nanofiltration*", Desalination, **Vol.343**, p.p.67–74, (2014).
12. Amin Maher, Morteza Sadeghi, Ahmad Moheb, "*Heavy metal elimination from drinking water using nanofiltration membrane technology and process optimization using response surface*

methodology", Desalination, **Vol.352**, p.p.166–173, (2014).
13. Xiuzhen Wei, Xin Kong, Songxue Wang, Hai Xiang, Jiade Wang, and Jinyuan Chen, "*Removal of Heavy Metals from Electroplating Wastewater by Thin-Film Composite Nanofiltration Hollow-Fiber Membranes*", Industrial & Engineering Chemistry Research, **Vol. 52**, p.p.17583−17590, (2013).
14. Ahmed Faiq Al-Alawy, "*Performance of Manipulated Direct Osmosis in Water Desalination Process*", Ph.D. Thesis, University of Baghdad, (2007).
15. Myzairah Binti Hamdzah, "*LOW PRESSURE REVERSE OSMOSIS MEMBRANE FOR REJECTION OF HEAVY METALS*", Msc. Thesis, University Teknologi Malaysia, (2007).
16. John C. Crittenden, R. Rhodes Trussell, David W. Hand, Kerry J. Howe, George Tchobanoglous, a book of "*MWH's Water Treatment Principles and Design*", published by John Wiley and Sons, Inc., third edition, p.p. 1335- 1414, (2012).
17. Jane Kucera, a book of "*Reverse Osmosis Design, Processes, and Applications for Engineers*", published by Scrivener Publishing LLC, p.p.41-84, (2010).
18. Woodyian N. Khudair, "*Reduction of Concentrating Poisonous Metallic Radicals from Industrial Wastewater by Forward and Reverse Osmosis*", Msc. Thesis, University of Baghdad, (2011).
19. Michael E. Williams, "*A Review of Reverse Osmosis Theory"*, Corporation and Williams Engineering Services Company, Inc., (2003).
20. Tamara Kawther Hussein, "*Forward Osmosis for Removal of Lead, Copper and Nickel from Aqueous Solutions*", Ph.D. Thesis, University of Baghdad, (2015).
21. Schock, G., and Miguel, A., "*Mass Transfer and Pressure Loss in Spiral Wound Modules*", Desalination, **Vol.64**, p.p. 339–352, (1987).
22. Belkacem Absar, Sid El Mahi Lamine Kadi and Omar Belhamiti, "*Mathematical Modeling of Reverse Osmosis Process by the Orthogonal Collocation on Finite Element Method*", Asian Journal of Applied Sciences, **Vol.1(1)**, p.p.1-18, (2008).
23. Jamal K., M. Khan and M. Kamil, "*Mathematical Modelling of Reverse Osmosis*", Desalination, **Vol.160**, p.p. 29–42, (2004).
24. Zhi Wang, Guangchun Liu, Zhifeng Fan, Xingtao Yang, Jixiao Wang, Shichang Wang, "*Experimental study on treatment of electroplating wastewater by nanofiltration*", Journal of Membrane Science, **Vol.305**, p.p. 185–195, (2007).
25. Kyu-Hong Ahn, Kyung-Guen Song, Ho-Young Cha, Ick-Tae Yeom, "*Removal of ions in nickel electroplating rinse water using low-pressure nanofiltration*", Desalination, **Vol.122**, p.p.77-84, (1999).
26. Xijun Chai, Guohua Chen, Po-Lock Yue, Yongli Mi, " *Pilot scale membrane separation of electroplating waste water by reverse osmosis*", Journal of Membrane Science, **Vol.123**, p.p.235-242, (1997).
27. Jae-Wok Lee, Tae-Ouk Kwon, Il-Shik Moon, "*Performance of polyamide reverse osmosis membranes for steel wastewater reuse*", Desalination, **Vol.189**, p.p. 309-322, (2006).